Received 00th January 20xx,
Accepted 00th January 20xx

DOI: 10.1039/x0xx00000x

On-surface synthesis of extended linear graphyne molecular wires by protecting the alkynyl group

Francesco Sedona,*[,a] Mir Masoud Seyyed Fakhrabadi,[a,b] Silvia Carlotto,[a] Elaheh Mohebbi,[a] Francesco De Boni,[a] Stefano Casalini[a], Maurizio Casarin[a] and Mauro Sambi*[,a,c]

In this paper we report on the use of an Ullmann-like aryl halide homocoupling reaction to obtain long Graphyne Molecular Wires (GY MW) organized in dense, ordered arrays. Instead of using highly reactive terminal alkynes, we resort to a precursor wherein the acetylenic functional group is internal, namely protected by two phenyl rings, each bearing a Br atom in para position to allow for linear homocoupling. In addition, two further factors concur to the production of dense and highly ordered arrays of very long GY MWs, namely the geometric compatibility between the substrate and both the organometallic intermediates and the final polymeric products of the synthesis, coupled with the presence of surface-adsorbed bromine atoms separating the MWs, which minimize secondary reactions leading to inter-wire cross-linking and consequently its disorder.

Introduction

Graphyne (GY) is a bi-dimensional theoretically predicted non-natural carbon allotrope characterized by the regular combination of C≡C triple bonds and phenyl groups, and therefore sp and sp^2 hybridized carbon atoms, according to a certain periodic rule.[1] The on-surface synthesis approach in recent years has shown a powerful potential in providing efficient synthetic routes to obtain GY nanostructures. [2,3,4]

The most promising results have been obtained with the synthesis of Graphyne Molecular Wires (GY MWs), characterized by the presence of phenyl rings and acetylenic linkages within the same wire. These can be classified as *m,n* GY MWs, where *m* is the number of phenyl rings and *n* is the number of alkyne moieties in the repeating monomer. The wires with two adjacent alkynyl moieties (*n*=2, butadiynylene groups) are generally called Graphdiyne molecular wires (GDY MW).[5]

In this scenario, some works obtained GDY MWs by employing the dehydrogenative homocoupling of terminal alkynes (Glaser coupling)[6,7] or the dehalogenative homocoupling of terminal alkynyl bromides (Ullmann coupling),[8,9,10] whereas GY MWs have been recently obtained by the direct in situ formation of triple C≡C bonds through the on-surface dehalogenative homocoupling of tribromomethyl-substituted arenes.[11,12] A more complex system has been produced and studied, starting from molecular linear precursors that combine terminal alkynes at one end and phenyl bromide on the other end: in this case three competitive reactions are involved (Glaser, Ullmann and Sonogashira couplings), producing both GY and GDY MW.[13]

In all these works the alkynyl units or their precursors are end-groups of the molecular monomer undergoing polymerization, this feature, coupled to the high reactivity of terminal alkynes, leads to poor chemo- and regio-selectivity of the polymerization reaction pathways, with several side reactions (cis/trans hydrogenation, insertion, cyclotrimerization, etc.) that ultimately lead to the formation of a mixture of short-chain, branched and irregular oligomers. A certain degree of control on the selectivity has been obtained by Klappenberger et al. in the low-coverage regime, by combining the templating effect of the Ag(455) stepped surface with the steric hindrance of the lateral carbonitrile groups added to the diethynyl-terphenyl precursor, resulting in linear chains with a maximum lengths of 40 nm.[7]

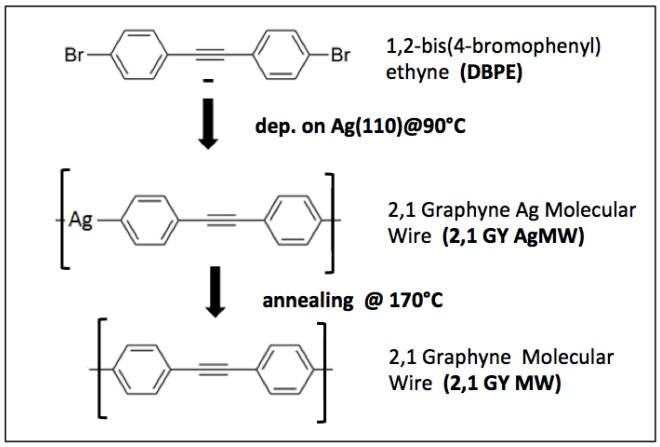

Figure 1. Schematic representation of longitudinal polymerization of **DBPE** molecules via an organosilver intermediate into a **2,1 GY MW**.

[a] *Dipartimento di Scienze Chimiche, Università Degli Studi di Padova, Via Marzolo 1, 35131 Padova, Italy.*
[b] *Current address: School of Mechanical Engineering, College of Engineering, University of Tehran, Tehran, Iran.*
[c] *Consorzio INSTM, Unità di Ricerca di Padova, Padova, Italy.*
Electronic Supplementary Information (ESI) available. See DOI: 10.1039/x0xx00000x

In this paper we show that the well-established Ullmann-like aryl halide homocoupling[14] reaction can be used to obtain surfaces with high coverage of long GY MWs organized in ordered arrays. Instead of using highly reactive terminal alkynes, we resort to 1,2-bis(4-bromophenyl) ethyne (**DBPE**) molecules (Figure 1) as molecular precursor, wherein the acetylenic functional group is internal rather than terminal, being linked to two phenyl groups, each bearing a Br atom in para position. As reported in Figure 1, **DBPE** deposited and annealed on Ag(110) leads to the production of linear **2,1 GY MWs** through a two-step synthesis involving the organosilver nanowire **2,1 GY AgMW** as an intermediate. Very recently a similar approach has been adopted by H. Shan et al., who obtained long GDY MW starting from a brominated precursor wherein the butadiynylene group is protected by two arynyl groups [15]

Methods

Sample Preparation. The Ag(110) and Ag(111) single crystals were cleaned by repeated cycles of 1 keV Ar^+ sputtering and annealing at 550 °C until a clean surface with large terraces was confirmed by XPS, STM imaging and LEED. Commercially available **DBPE** molecules (Aldrich) were deposited from a pyrolytic boron nitride crucible held at ~80 °C. The molecular source was outgassed until the pressure stopped to increase during the sublimation. Molecular beam deposition was performed on the substrate held at 90 °C for 10 minutes

STM Imaging. Experiments were performed in UHV at a base pressure of 2×10^{-10} mbar in an Omicron VT-STM. The measurements were carried out at RT in constant-current mode using an electrochemically etched Pt–Ir tip. The STM data were processed with the WSxM software.[16] Moderate filtering was applied for noise reduction. Sample bias values are reported throughout the article.

X-ray Photoelectron Spectroscopy. Measurements were performed in situ at RT using a VG Scienta XM 650 Al Kα X-ray source (1486.7 eV) and a VG Scienta XM 780 monochromator. Photoelectrons were collected with a Scienta SES 100 electron analyzer fitted to the STM preparation chamber.

Simulations. Theoretical results were obtained by periodic DFT calculations using the Quantum-ESPRESSO package[17] and by adopting the Perdew-Burke-Ernzerhof exchange–correlation functional.[18] Valence orbitals were expanded in a plane-wave basis set with a kinetic energy cutoff of 30 Ry, while the interaction between ion cores and valence electrons has been modeled by means of ultrasoft pseudopotentials.[19] The cutoff on the charge density was 240 Ry. Brillouin-zone integrations were limited to the gamma-point and a smearing parameter of 0.02 Ry for the electron population function was considered.[20] Numerical experiments have been carried out with and without the inclusion of the dispersion corrections (by means of the Grimme method).[21,22] STM images have been modeled by using the Tersoff-Hamann approximation.[23]

Results and Discussions

Figure 2a reports a large scale STM image after a 10 minutes deposition of **DBPE** on Ag(110) held at 90 °C: the surface is completely covered by an ordered array of molecules organized in two separate domains (highlighted by blue arrows) that give a Low Energy Electron Diffraction (LEED) pattern, compatible with a commensurate superlattice expressed by the $[3 \pm 1, -2 \pm 3]$ matrix notation (see Figure S1a in the supporting information, SI). The molecular modelization of this structure takes into account the well-documented formation of organometallic structures on silver and copper surfaces starting from halogenated molecules and leading to linear and bi-dimensional structures.[24,25] Figure 2b shows that the high-resolution STM image is, in fact, well-reproduced by the Tersoff-Hamman STM simulation derived from the Density Functional Theory (DFT) proposed model (for computational details see SI) where the bromine atoms (red spots) detach from opposite ends of **DBPE** and silver adatoms (blue spots) replace them, thereby creating the organosilver **2,1 GY AgMWs** aligned along the $[1\bar{1}3]$ and $[\bar{1}13]$ symmetry-equivalent surface directions, in agreement with the LEED pattern. This alignment is guided by the approximate coincidence between the self standing organometallic repetition unit length, that is calculated to be 13.8 Å, and the $[1\bar{1}3]$ substrate unit vector that is 13.53 Å long, with a small mismatch of about 1.9%, therefore MWs are not aligned along the principal directions of the surface because this geometry would cause a mismatch of 4.6%. A similar behavior has been already reported on comparable systems, such as poly(para-phenylene) (PPP) on Cu(110).[26,27] The dissociated bromine atoms remain adsorbed on the silver substrate on two precisely identifiable positions: between two silver adatoms belonging to adjacent organosilver wires and in the free space between two nearby C≡C triple bonds (denoted by A and B in Figure 2b). The DFT simulation well reproduces the brightness variation between A and B bromine atoms, which is correlated with the different absorption site they occupy on the silver substrate, with B (darker) bromine atoms on long-bridge positions, and with the A (brighter) ones on-top of Ag substrate atoms (see Figure 2B).

The second step of the synthesis consists of annealing the surface at 170°C for at least 45 minutes to obtain a fully covered and ordered surface, as shown by the large scale STM image in Figure 2c. This thermal treatment is performed under deposition flux of **DBPE** to contrast the molecular desorption from the surface, a similar desorbtion has been already reported for a pyrene organo-silver nanostructure on Ag(111),) even though the mechanistic details are still not clear.[28]

Aiming to obtain a well-ordered final covalent structure, it is critical to pass trough a well-ordered organometallic structure: the direct deposition of molecules at 170°C leads to the formation of small domains composed by only a few monomers. The high-resolution STM images (left part of Figures 2d) confirms the release of the silver adatoms because of the thermal treatment causes yielding the formation of molecular wires characterized by the regular repetition of a monomer of about 1.1 nm length, compatible with the formation of **2,1 GY MWs**. Indeed, the STM contrast of the

organic part is well reproduced by the DFT simulation reported in Figure 2d (central part), where the C≡C triple bond corresponds to a reduced width of the organic wire and the two phenyl rings to two rounded shapes, whereas the bromine atoms are still in-between the nanowires. The LEED pattern does not show any clear sign of commensuration of the polymer with the substrate, but reveals that in average the bromine atoms form a $[3 \pm 1, -1 \pm 1]$ unit cell, as reported in Figure S1b. Accordingly, polymeric wires are aligned on average along the $[1\bar{1}2]$ and $[\bar{1}12]$ directions and hence rotated by 10° with respect to the organometallic wires. To simulate the surface structure, a large unit cell aligned along $[1\bar{1}2]$ has been considered, as reported in the right part of Figure 2d, wherein the Br atoms give rise to the smaller unit cell compatible with LEED. The organic nanostructure shows a higher density of surface-adsorbed Br atoms with respect to the organometallic overlayer (the increase is around 10%), which is compatible with the long annealing treatment realized under **DBPE** evaporation and therefore with the possibility to accumulate Br atoms, but we cannot exclude that some spots between the MWs could be assigned to the silver adatoms belonging to the previous organometallic MWs.[15]

Further information on the reaction sequence as a function of temperature is provided by XPS measurements: results for C 1s and Br 3d normalized peaks from the two synthesis steps are compared in Figure 3. Both the Br 3d peaks have the 5/2 component centered at 68.0 eV (Figure 3a), confirming that Br atoms are adsorbed at the surface. It is interesting to note that for the **2,1 GY MW** a good fitting can be obtained only by adding a small component at +0.7 eV with respect to the main feature. This component has been recently reported when studying the role of halogens in Ullmann coupling and has been tentatively attributed to different adsorption sites of the halogen atoms within the organic structure.[29]

The C 1s peak shifts from a BE of 284.3 eV for the organosilver wires, characterized by the C-Ag bonds, to 284.5 eV after the annealing at 170 °C and the release of the Ag atoms with the formation of direct C-C bonds.[30] This effect is well visible from the Löwdin charge analysis of the DFT optimized models, where the organosilver **2,1 GY AgMW** is negatively charged with respect to the covalent **2,1 GY MW** for a total amount of 0.862 electron charge units (see Table S1 in the SI).

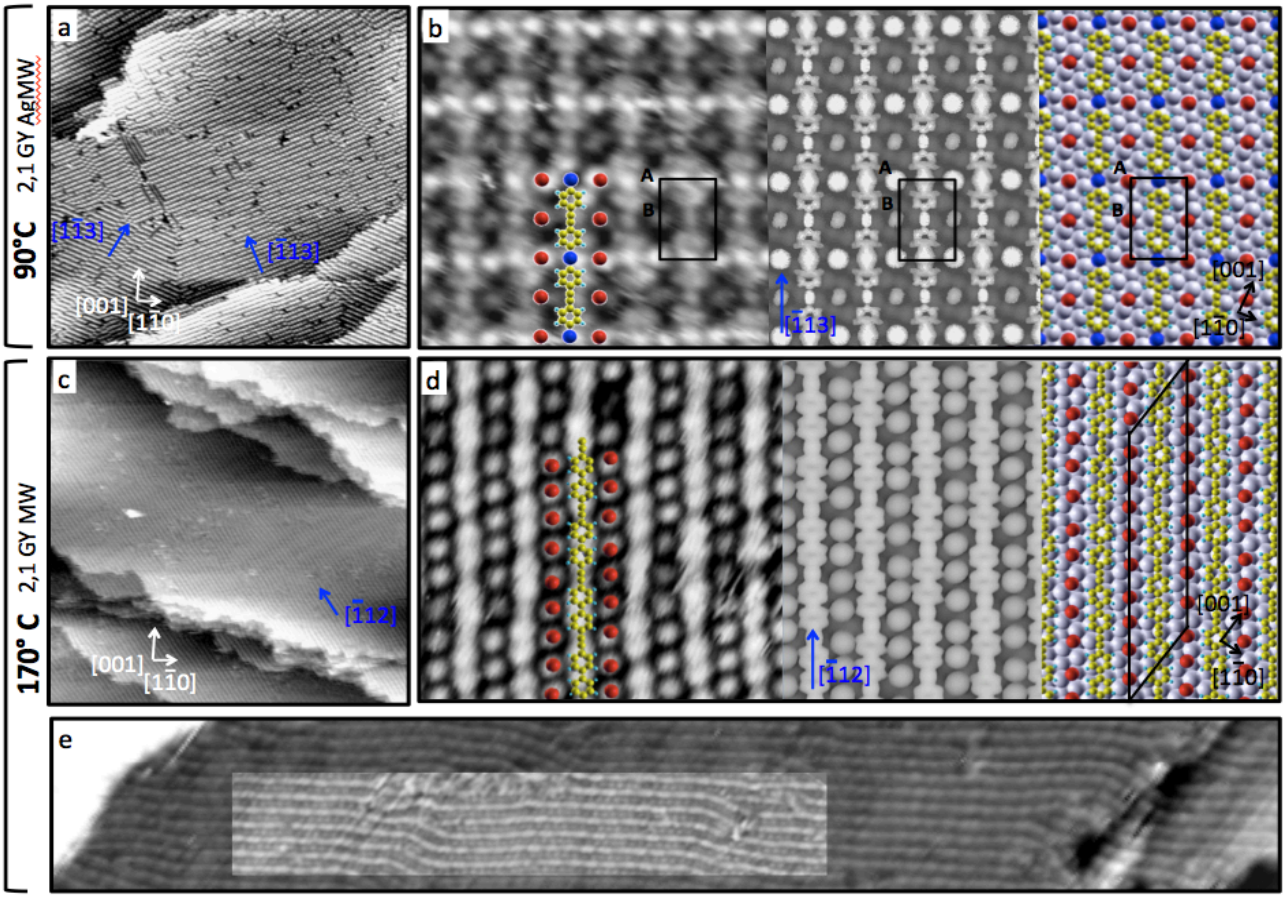

Figure 2: **2,1 GY AgMWs** obtained after deposition of DBPE on Ag(110) kept at 90 °C **a)** large scale experimental STM image (100×100 nm², V = -1 V, I = 1.3 nA), **b)** comparison between the experimental high-resolution image (V=-0.7 V, I=12 nA 6x6 nm²) (*left*) and the simulated image (*center*) obtained from the DFT calculated model (*right*) (Br red, C yellow, H light blue, Ag adatoms dark blue, Ag substrate grey, while the black rectangle outlines the $[3 \pm 1, -2 \pm 3]$ unit cell and A and B outline the two different adsorbed Br atoms).
2,1 GY MWs obtained after annealing at 170 °C. **c)** large scale experimental STM image (100×100 nm², V = 0.2 V, I = 4.3 nA), **d)** comparison between the experimental high-resolution image (V=-1 V, I=12 nA 6x6 nm²) (*left*) and the simulated image (*center*) obtained from the DFT calculated model (*right*), where the unit cell is outlined by a black line.(Br red, C yellow, H light blue, Ag substrate grey). **e)** Collage of two experimental STM images (large 100×12 nm² small 49x 7,4 nm², both V=-0.6 V and I=0.3 nA) to show the typical length and the continuity of **2,1 GY MWs**.

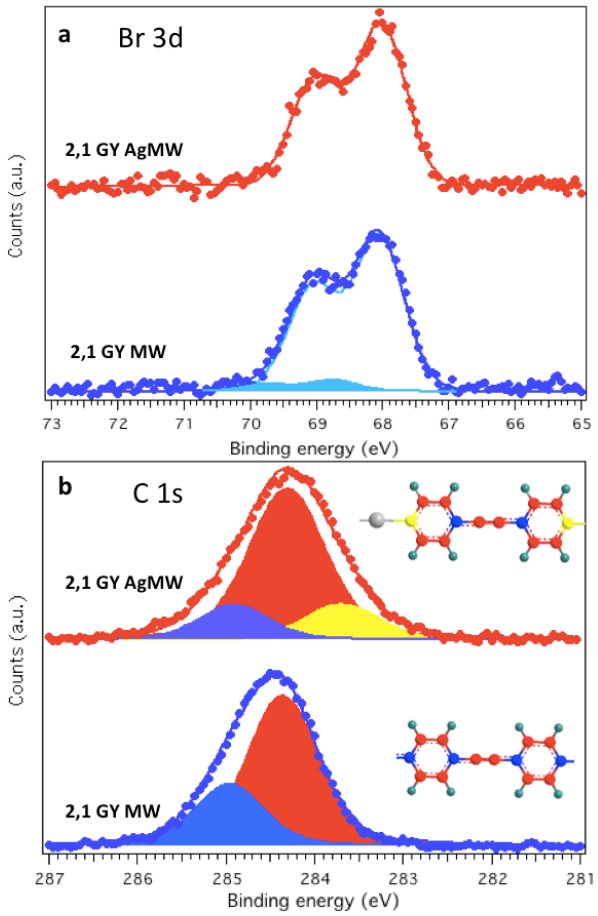

Figure 3 Experimental peaks and fitting of (a) Br3d and (b) C1s XPS peaks of the organosilver **2,1 GY Ag MW** obtained after annealing at 90 °C and of the **2,1 GY MW** obtained after annealing at 170 °C on Ag(110). MW models evidence with different colors the carbon species that contributes to the XPS signal with different contribution

In agreement with the previous literature on alkynes structures supported on silver surfaces, the **2,1 GY AgMW** C 1s peak can be fitted with three components: the main peak at 284.2 eV is attributed to C-H and alkynes carbon atoms (red), the C atoms directly linked to the silver adatoms (yellow) are responsible for the low binding energy component at 283.6 eV, whereas the sp^2 hybridized C atoms directly linked to other three C atoms (blue) are responsible of the high binding energy component at 284.7 eV. The areas of the three components perfectly reflect the abundance of the three species in the organometallic wires.[31,32] The formation of the **2,1 GY MW modifies** the C atoms bonded to the metal into C atoms linked to three C atoms; the resulting XPS region can now be fitted with just the two red and blue components, that substantially maintain the same positions reported for the organometallic wires.

Thanks to the synthetic strategy proposed in this work, we obtained a long-range ordered, dense array of separated GY MWs with lengths that can easily reach 100 nm, as reported in Figure 2e, which shows that the polymers can cross the surface steps, and can bend from linearity by small angles, in tune with the flexibility of similar molecular wires such as PPP.

Among the previous works on GY/GDY MWs, only Klappenberger et al.[7] analyzed the MW defects level, revealing that in the best scenario (i.e. by using laterally functionalized monomers on stepped surfaces at low coverage) a level of 93% of "right" linear connections between the monomers can be obtained. In our case a statistical evaluation of a large number of STM images shows that we can estimate a level of >97% of linear connections on a fully covered surface.

The dimensions and the defectivity of the nanostructures and specifically of the molecular wires are key points for future device construction and it is therefore important to rationalize the main factors that influence these structural results. In our case we analyzed three main factors: (1) the reactivity of the precursor, (2) the geometric compatibility between the substrate and the intermediate as well as the final nanostructures and (3) the effect of the reaction by-products and of surface adatoms on the reaction outcome.

1) As already mentioned, in the **DBPE** precursor the highly reactive alkynyl group is in the central position, protected by two phenyl rings. This approach seems to lead to less defective molecular wires compared with the one that uses precursors that expose the alkynyl group at the apex. More specifically, very recently two works obtained the same **2,1 GY MW** reported in our work starting from precursors with apical alkynyl groups and obtained a lower level of chemo- and regio-selectivity, leading to a more defective final result. In particular, the synthesis performed by Wei Xu et al. has been supported on Ag(110) and is therefore directly comparable with our results. [13, 33] Very recently, the same principle has been additionally confirmed by H. Shan et al., who obtained long 2,2 GDY MW starting from a brominated precursor wherein the butadiynylene group is protected by two aryl groups.[15]

2) As in other cases,[34] and in particular in the case of poly(para-phenylene) (PPP) MWs on Au(111),[35] in order to obtain a lowly defective covalent structure, it is necessary to pass through an intermediate structure that fits two requirements: a high level of order obtained thanks to reversible interactions between the building units, and a geometric compatibility between this intermediate structure and the final covalent structure. In this work the organometallic structure fulfills both these requisites. Indeed, as already reported in the literature,[36] the organometallic structures can reach a high level of order due to the C-metal bond reversibility. As reported in the two models in Figure 2, both the organometallic wires and the covalent polymers obtained after annealing at 170 °C are aligned along similar directions and therefore the latter can be obtained from the former only by the expulsion of silver adatoms and a small rotation of about 10°. The key role of the substrate geometry is evidenced by comparing the results obtained on Ag(110) with the ones obtained on Ag(111) in similar reaction conditions. Figure 4a reports the STM image after the deposition of DPPE on Ag(111) held at 90°C. Although also in this system Br is initially substituted by Ag, adatoms as confirmed by the XPS analysis reported in Figure S2, this intermediate structure does not organize in molecular wires, but rather in individual organometallic molecules showing a LEED pattern in agreement with a [5 2, 0 5] unit cell, as reported in figure S3. After the annealing at 170°C the surface rearranges forming **2,1 GY MW** oriented along the $\langle 1\bar{2}1 \rangle$ directions, as reported in Figure 4b. It is evident that – due to the difference between the starting organometallic structure and the final covalent geometry – this reaction implies a substantial surface mass transport, resulting in the formation of small islands of **2,1 GY MW** oligomers and a large amount of defective interconnections. The lack of organometallic molecular wires can be explained by the rather large mismatch (minimum 4.2%) between the length of the **2,1 GY AgMW** repetition unit (13.4 Å) and any substrate lattice parameter.

3) An important role in the successful outcome of the synthetic strategy is also played by Br atoms detached from **DBPE** in the first step of the Ullmann-like synthesis. By residing on the substrate, they keep apart the growing MW with a twofold effect: they both (i) direct the linear growth of the polymeric chains and (ii) limit the access to (i.e. protect) the alkynyl groups within the chain, thereby substantially enhancing the reaction's chemo/regioselectivity by preserving its essentially topotactic nature. H. Shan et al. report that a similar effect can be also played by Au adatoms positioned near to the butadiynylene group in their precursor, which protect the triple bonds from reactions with other radicals.[15]

This effect is particularly evident at temperatures higher than 320°C when Br atoms start to desorb as reported in Figure 5a where the MW maintain the uniaxial order as long as bromine atoms stay in place (blue arrow), but they start to degrade as soon as Br leaves the surface (yellow arrow). In still ordered areas yellow circles evidence x-shaped links between adjacent MWs that seem to point to a [2+2] cycloaddition[38,39] of two alkynyl groups belonging to adjacent wires as a starting point of the degradation process. However, given the complex chemistry of alkynes, which can undergo metathesis, insertion, cyclization, hydrogenation reactions to name but a few, the onset of Br desorption is generally accompanied by a degradation of the starting order that cannot be attributed unambiguously to a single dominant reaction scheme. In any case, the ultimate result is the formation of small oligomers linked in many different geometries.

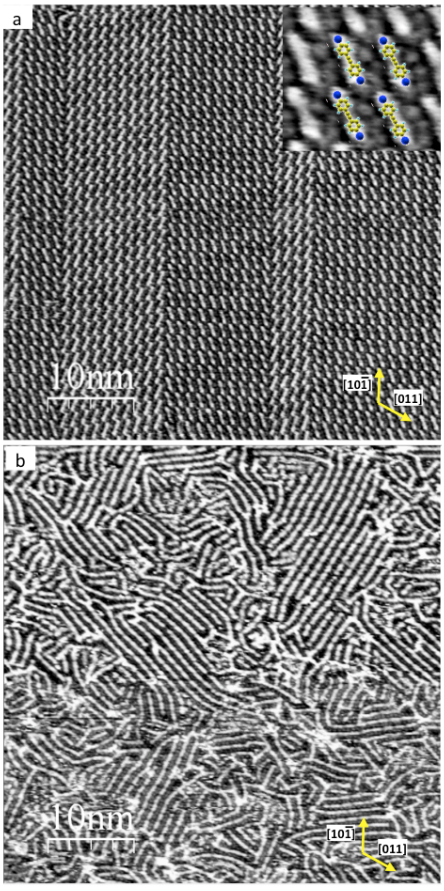

Figure 4 STM images a) (50 × 50 nm^2 ,V = -0.1 V, I = 3.7 nA) of **DBPE** deposited on Ag(111) kept at 90°C. Inset: zoom in with superimposed organometallic molecular model; b) (50×50 nm^2 ,V = 0.4 V, I = 3.5 nA) of polymers obtained after annealing at T=170 °C.

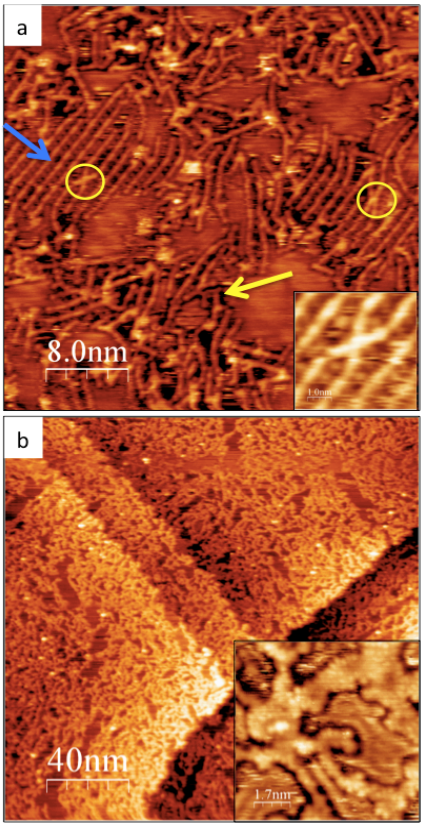

Figure 5: STM images. (a) (40 × 40 nm^2, V = 1.5 V, I = 0.2 nA) onset of the 2D linking of MW on Ag(110) (T=320°C): the blue arrow shows ordered nanowires and blue arrow a degraded zone, yellow circles indicate x-shaped links between adjacent nanowires that is zoomed in the inset; (b) (200 × 200 nm2, V = -0.7 V, 0.3 nA) and (b) (24 × 24 nm2, V = 0.8 V, I = 8 nA) 2D **DBPE**-based amorphous polymers (T=350°C), inset report a detail of the same surface (14x14 nm^2 V= 0.8V I=8 nA).

Further information about the role of surface- adsorbed Br atoms can be obtained by comparing the Löwdin charge analysis of the **2,1 GY AgMWs** and the **2,1 GY MWs** with and without Br atoms (see Table S1 in the SI). In both cases the charge on C atoms is the same, indicating that the bromine atoms negligibly affect the charge distribution. This result indicates that Br atoms play a "physical" (spacer) rather than a "chemical" (electronic interaction) role, thus preventing the interaction between nearest neighbour triple bonds and collectively playing the role of a "rail" for the longitudinal self-assembly of the wires. This explanation can be applied also to previous works on the characterization of PPP MWs, where the presence/absence of adsorbed Br atoms between MWs does not seem to influence their electronic features.[37]

In addition, Figures 5b shows that annealing at 350°C, when Br atoms completely desorb, leads to lateral reactions between the nanowires on the whole surface. The final result is an amorphous bi-dimensional short-branched mesh with no preferential growth direction compared to the starting ordered wires array. It is instructing to compare this finding with what has been observed starting from 4,4''-dibromo-p- terphenyl molecules, where no triple bonds are present: the PPP polymers are still intact after Br desorption and the graphene nanoribbons developing by their lateral fusion display a clear azimuthal orientation reminiscent of the order of starting PPP MWs.[35]

Interestingly, the optimized DFT polymeric chain structure shows that biphenylene units within the chain lie flat on the Ag(110)

surface, i.e. the dihedral angle both between nearest neighbour phenyl rings within a biphenyl unit and between successive biphenyl units is zero within ±2° (see the side views in Figure S7 in the SI). This behaviour is different from what is found for PPP wires supported on weakly interacting Au(887),[37] where the dihedral angle between successive phenyl rings was measured to be 40±10°, and similar to PPP on the much more strongly interacting Cu(110).[26] In that case, the twisted conformation of the para-linked phenylene units is due to the steric hindrance between the orto hydrogen atoms of neighbouring phenyl rings, which is counteracted by the vertical polymer-substrate interaction. Such steric hindrance in **2,1 GY MWs** is halved with respect to PPP due to the insertion of ethynyl spacers among biphenylene units. The resulting flat conformation maximizes the 1D polymer conjugation and should therefore reduce the optical band gap with respect to twisted conformations. The DFT HOMO-LUMO separation of unsupported **2,1 GY MW**, calculated for a molecule with 16 phenyl rings to prevent the dependence of the electronic structure from the length of the oligomer, amounts to 1.79 eV at the Γ point of the first Brillouin zone, which is reduced to 1.49 eV for the surface-supported polymeric wire.

In conclusion, in this paper we have shown that a long-range ordered, dense array of highly linear and extremely long graphyne molecular wires can be efficiently grown by adopting a synthetic strategy that preserves the reactive alkynyl group. The molecular protection is mainly due to three factors: 1) the acetylenic functional group is internal rather than external, thereby being linked to two phenyl groups; 2) the formation of the reversible organosilver intermediate at low temperature leads with only small adjustments to the final **2,1 GY MWs** and 3) the surface-adsorbed Br atoms act as spacers between adjacent organosilver nanowires, thus avoiding the interaction between adjacent C≡C triple bonds.

The research leading to these results has received funding from the European Commission, Seventh Framework Program (Grant Agreement no. 600376) and from the University of Padova (Grant CPDA154322 AMNES and Grant P-DISC#09BIRD2019-UNIPD SMOW)

Conflicts of interest

"There are no conflicts to declare".

Notes and references

[1] Y. Li, L. Xu, H. Liu, Y. Li, *Chem. Soc. Rev.*, 2014, ***43*(8)**, 2572.

[2] F. Kang, W. Xu, *ChemPhysChem*, 2019, **20**, 2251.

[3] J. Liu, Q. W. Chen, K. Wu, *Chinese Chemical Letters*,2017, ***28*(8)**, 1631.

[4] F. Klappenberger, Y. Q. Zhang, J. Björk, S. Klyatskaya, M. Ruben, J. V. Barth, *Accounts of chemical research*, 2015, ***48*(7)**, 2140.

[5] X. Li, H. Zhang, L. Chi *Advanced Materials*, 2018, 1804087.

[6] B. Cirera, Y.-Q. Zhang, J. Björk, S. Klyatskaya, Z. Chen, M. Ruben, J. V. Barth, F. Klappenberger, *Nano Lett.* 2014, ***14***, 1891.

[7] F. Klappenberger, R. Hellwig, P. Du, T. Paintner, M. Uphoff, L. Zhang, T. Lin, B. Abedin Moghanaki, M. Paszkiewicz, I.Vobornik, J. Fujii, O. Fuhr, Y.-Q. Zhang, F. Allegretti, M. Ruben, J. V. Barth, *Small* 2018, **14**, 1704321.

[8] J. Liu, Q. Chen, L. Xiao, J. Shang, X. Zhou, Y. Zhang, Y. Wang, X. Shao, J. Li, W. Chen, G. Q. Xu, H. Tang, D. Zhao, K. Wu, *ACS Nano* 2015, **6**, 6305.

[9] Q. Sun, L. Cai, H. Ma, C. Yuan, W. Xu, *ACS nano* 2016, **10(7)**, 7023.

[10] A. Rabia, F. Tumino, A. Milani, V. Russo, A. L. Bassi, S. Achilli, G. Fratesi, G. Onida, N. Manini, Q. Sun, W. Xu, C. S. Casari, *Nanoscale* 2019, **11**, 18191.

[11] C. H. Shu, M. X. Liu, Z. Q. Zha, J. L. Pan, S. Z. Zhang, Y. L. Xie ,P. N. Liu, *Nature Comm.* 2018, **9(1)**, 2322.

[12] Q. Sun, X. Yu, M. Bao, M. Liu, J. Pan, Z. Zha , W. Xu, *Angew. Chemie Int. Ed.* 2018, **57(15)**, 4035.

[13] T. Wang, J. Huang, H. Lv, Q. Fan, L. Feng, Z. Tao, J. Zhu, *J. Am. Chem. Soc.* 2018, **140(41)**, 13421.

[14] J. Eichhorn, D. Nieckarz, O. Ochs, D. Samanta, M. Schmittel, P. J. Szabelski, M. Lackinger, *ACS Nano* 2014, **8**, 7880.

[15] H. Shan, Y. Mao, A. Zhao *Chinese J. Chem. Phys.* 2019, **32(5)**, 620.

[16] I. Horcas, R. Fernández, *Rev. Sci. Instrum.* 2007, ***78***, 013705.

[17] P. Giannozzi, S. Baroni, N. Bonini, M. Calandra, R. Car, C. Cavazzoni, D. Ceresoli, G. L. Chiarotti, M. Cococcioni, I. Dabo, et al. *J. Phys. Condens. Matter* 2009, **21**, No. 395502.

[18] J. P. Perdew, K. Burke, M. Ernzerhof, *Phys. Rev. Lett.* 1996, **77**, 3865-3868.

[19] D. Vanderbilt,. *Phys. Rev. B* 1990, ***41***, 7892-7895.

[20] N. Marzari, D. Vanderbilt, A. De Vita, M. C. Payne, *Phys. Rev. Lett.* 1999, **82**, 3296-3299

[21] S. *J.* Grimme, *Comput. Chem.* 2006, **27**, 1787-1799.

[22] V. Barone, M. Casarin, D. Forrer, M. Pavone, M. Sambi, A. Vittadini, *J. Comput. Chem.* 2009, **30**, 934-939.

[23] J. Tersoff, D. R.Hamann, *Phys. Rev. Lett.* 1983, **50**, 1998-2001.

[24] K. H. Chung, B. G. Koo, H. Kim, J. K. Yoon, J. H. Kim, Y. K. Kwon, S. J. Kahng, *Phys. Chem. Chem. Phys.* 2012, ***14***, 7304.

[25] Q. Fan, L. Liu, J. Dai, T. Wang, H. Ju, J. Zhao, J.Kuttner, G. Hilt, J. M. Gottfried, J.Zhu, *ACS Nano* 2018, **12**, 2267.

[26] G. Vasseur, Y. Fagot-Revurat, M. Sicot,; B. Kierren, L. Moreau, D. Malterre, L. Cardenas, G. Galeotti, J. Lipton-Duffin, F. Rosei, *Nat. Commun.* 2016, **7**, 10235.

[27] M. Abyazisani, J. M. MacLeod, & J. Lipton-Duffin *ACS nano* 2019, ***13*(8)**, 9270.

[28] M. Lischka, M. Fritton, J. Eichhorn, V. S. Vyas, T. Strunskus, B. V. Lotsch, J. Bjork, W. M. Heckl, M. Lackinger, *J. Phys. Chem. C* 2018, ***122*(11)**, 5967.

[29] G. Galeotti, M. Di Giovannantonio, J. L. Duffin, M. Ebrahimi, S. Tebi, A. Verdini, L. Floreano, Y. F. Revurat, D. F. Perepichka, F. Rosei, G. Contini, *Faraday Discussion* 2017, **204**, 453.

[30] I. Píš, L. Ferrighi, T. H. Nguyen, S. Nappini, L. Vaghi, A. Basagni, E. Magnano, A. Papagni, F. Sedona, C. Di Valentin, S. Agnoli; F. Bondino, *J. Phys. Chem. C* 2016, **120**, 4909.

[31] T. Wang,H. Lv, J. Huang, H. Shan, L. Feng, Y. Mao, J. Wang, W. Zhang, D. Han, Q. Xu, P. Du, A. Zhao, X. Wu S. L. Tait, J. Zhu, *Nat. Comm.* 2019, **10,** 4122.

[32] Y.-Q. Zhang, N. Kepcija, M. Kleinschrodt, K. Diller, S. Fischer, A. C. Papageorgiou, F. Allegretti, J. Bjork, S. Klyatskaya, F. Klappenberger, M. Ruben, J. V. Barth, *Nat. Comm.* 2012, **3(1)**, 1.

[33] X. Yu, L. Cai, M. Bao, Q. Sun, H. Ma, C. Yuan, W. Xu, *Chem. Comm.* 2020, **56(11)**, 1685.

[34] J. Eichhorn, T. Strunskus, A. Rastgoo-Lahrood, D. Samanta, M. Schmittel, M. Lackinger, *Chem. Comm.* 2014,***50*(57)**, 7680.

[35] A. Basagni, F. Sedona, C. A. Pignedoli, M. Cattelan, L. Nicolas, M. Casarin, M. Sambi, *J. Am. Chem. Soc.* 2015, 137, 1802-1808.

[36] Y. Q. Zhang, T. Paintner, R. Hellwig, F. Haag, F. Allegretti, P. Feulner, & F. Klappenberger, *J. Am. Chem. Soc.* 2019, ***141*(13)**, 5087.

[37] A. Basagni, G. Vasseur, C.A. Pignedoli, M. Vilas-Varela, D. Peña, L. Nicolas, L. Vitali, J. L. Checa, D. G. Oteyza, F. Sedona, M. Casarin, J. E. Ortega, M. Sambi, *ACS Nano* 2016, **10**, 2644.

[38] B. V. Tran, T. A. Pham, M. Grunst, M. Kivala, M. Stöhr, *Nanoscale* 2017, **9**, 1805.

[39] N. E. Schore, *Chem. Rev.* 1988, **88**, 1081.